Chitosan Nanoparticle - Montmorillonite - Titanium Dioxide Nanocomposites: Synthesis, Characterization, and Antimicrobial Activity

Eswaran, Amutha
Sri Paramakalyani Centre of Excellence in Environmental Sciences, Manonmaniam Sundaranar University, Alwarkurichi - 627412, INDIA

Subramanian, Rajaduraipandian; Sivasubramanian, Gandhimathi
Sri Paramakalyani College, Manonmaniam Sundaranar University, Alwarkurichi – 627412, INDIA

Gurusamy, Annadurai *+
Sri Paramakalyani Centre of Excellence in Environmental Sciences, Manonmaniam Sundaranar University, Alwarkurichi - 627412, INDIA

ABSTRACT: *In recent years, a strong interest has emerged in hybrid composites and their potential uses, especially in Chitosan Nanoparticle – MontMorillonite - Titanium dioxide - (CSNP – MMT - TiO_2) composites, which have interesting technological properties and applications. Using the Precipitation Method, Chitosan Nanoparticles with TiO_2 Nanocomposite (CSNP – MMT - TiO_2 Nanocomposite) was created. Analysis using Scanning Electron Microscopy (SEM) revealed that the modified TiO_2 Nanocomposite was successfully dispersed into the Chitosan matrix and that the roughness of the Chitosan Nanoparticle - MMT- TiO_2 Nanocomposites were significantly reduced. Moreover, X-Ray Diffraction (XRD) and Fourier Transform InfraRed (FT-IR) spectroscopy analyses indicated that the Chitosan interacted with TiO_2 Nanocomposite and possessed good compatibility, while a ThermoGravimetric Analysis (TGA) of the thermal properties showed that the Chitosan-MMT-TiO_2 Nanocomposites with 0.05% TiO_2 Nanocomposite concentration had the best thermal stability. The Chitosan- MMT-TiO_2 Nanocomposite exhibited an inhibitory effect on the growth of gram-positive and gram-negative microorganisms.*

KEYWORDS: *Chitosan; Precipitation method; Chitosan Nanoparticle–Montmorillonite - titanium dioxide Nanocomposites; Thermal stability; Antibacterial activity*.

INTRODUCTION

Nanoscale materials are structures ranging from 1 to 100 nm, as defined in the chemistry context, which has contributed to the development of Nanoscience and nanotechnology at an exponential rate in recent years [1]. World's urgent need is to develop a new class of composite materials that physically integrates inorganic catalytic

** To whom correspondence should be addressed.*
+ E-mail: gandhicichu@gmail.com & gannadurai@msuniv.ac.in
1021-9986/2023/1/19-26 8/$/0.08

NanoParticles (NPs) and biologically active molecules which can replace antibiotics and be effective against resistant bacterium [2].

Chitosan is a linear polysaccharide, produced usually by deacetylation of chitin, which is the structural element in the exoskeleton of crustaceans (crabs, shrimp, etc.) [3]. Due to its special structure containing many functional groups such as aminyl or hydroxyl, it has a tendency to form complexes with metals[4,5]. Chitosan (poly-β-(1→4)N-acetyl-D-glucosamine) is a natural macromolecule polysaccharide[6], which has broad applications in the preservation of fruit and vegetables[7], due to its properties of film-forming[8], biocompatibility [9], low toxicity[10], antimicrobial activity[11]. Chitosan also has anti-bacterial properties which can be used as an additional function in titania and Chitosan composites. Antibacterial Chitosan involves the interaction between Chitosan molecules that are positively charged with a negatively charged bacterial membrane [12]. The internal osmotic imbalance of bacterial cells is due to changes in the permeability properties of bacterial cell membranes thereby inhibiting bacterial cell growth [13]. Chitosans itself comes from the skin of crustacean living things and is often found in the fishing industry[14].

TiO_2 is extensively used in several industrially relevant processes, in systems ranging from environmental applications to clean energy and from cosmetics to paint [15,16]. The wide use of TiO_2 is based on its exceptionally efficient photo activity, high chemical stability, biomedical applications and low cost [17].

Montmorillonite is the most common and the best-studied clay, which has been used in polymer nanocomposites for almost three decades. *Montmorillonite* belongs to the smectite family of clays and it has 2:1 layer structure, which means that the structure unit of *Montmorillonite* consists of two tetrahedral silica layers separated by an octahedral alumina layer [37 -40].

Therefore, the objective of this study was to explore the feasibility of producing antibacterial Chitosan Nanoparticle – Montmorillonite - Titanium Dioxide Nanocomposite using sol-gel and precipitation methods. The physicochemical properties of *Chitosan Nanoparticle – Montmorillonite - Titanium Dioxide* Nanocomposite were investigated by Scanning Electron Microscopy (SEM), X-Ray Diffraction (XRD), Fourier Transform InfraRed Spectroscopy (FT-IR), UV spectroscopy (UV), Particle Size Analyser (PSA) and ThermoGravimetric Analysis (TGA) techniques. In addition, the antimicrobial activity of the newly synthesized CSNP-MMT-TiO_2 Nanocomposite was tested against five bacterial (*Escherichia coli, Enterobacter, Psedomonous, Bacillus subtillus and Staphylococcus aureus*) species.

EXPERIMENTAL SECTION

Materials

The chemicals used to synthesis CSNP-MMT-TiO_2 Nanocomposite are Chitosan Analytical Grade (De-acetylation degree >75%),, Glacial acetic acid (CH_3COOH), sodium tripolyphosphate, Titaniam dioxide and K-10 montmorillonite (MMT). All the chemicals and reagents are from Himedia brand with 99.9% purity which is used here without further purification. Bacterial isolates, Gram-positive *staphylococcus aureus and Bacillus subtilus*, and Gram-negative *Escherichia coli*, *Enterobacter and Pseudomonas fluorescens* were procured from standard vendors.

Synthesis of chitosan nanoparticle

Chitosan nanoparticle from Chitosan was manufactured through the method “IONIC GELATION”. This involves the ionic interaction of 2.4g of Chitosan in 6 mL of acetic acid with 594 mL of distilled water. This forms the Chitosan emulsion. Further, the emulsion is allowed to dissolve well which was then titrated with 4.06g of anionic sodium tripolyphosphate (STPP) dissolved in 400mL distilled water. The mixture is simultaneously mixed through a magnetic stirrer. The final product, the micro gel was obtained which was later frozen at 4° C for 24 hours which was then filtered and dried at 60 °C. the final product obtained was powdered using mortar and pestle. The white powder obtained was known as a Chitosan nanoparticle.

Synthesis of CSNP-MMT nanocomposites

0.5g of Chitosan nanoparticle was mixed with distilled water (100 mL) and 0.5g of Montmorillonite was added to the above solution. The reaction was maintained at constant stirring. 5% of acetic acid was added dropwise. The reaction was maintained for about 2-4 hrs. Sodium tripolyphosphate was added to the above solution and it was allowed to stir for 12 hrs. Then it was subjected to centrifugation for 30 min. and was dried in a hot air oven at 100°.

The obtained powder was grinded using mortar and pestle and subjected to calcination for 800°. Now the CSNP-MMT Nanocomposite was synthesized.

Synthesis of CSNP-MMT/TiO₂ nanocomposite

To make a Nanocomposite, finally, 0.5g of CSNP-MMT Nanocomposite was taken and mixed with distilled water (100 mL), and 0.5g of Titanium dioxide (TiO_2) was added to the above solution. The reaction was maintained at constant stirring. 5% of acetic acid was added dropwise. The reaction was maintained for about 2-4 hrs. Sodium tripolyphosphate was added to the above solution and it was allowed to stir for 12 hrs. Then it was subjected to centrifugation for 30 min. and was dried in a hot air oven at 100°. The obtained powder was ground using mortar and pestle and subjected to calcination for 800°. Finally, the CSNP-MMT/TIO_2 Nanocomposite was synthesized.

Antibacterial property

Agar well diffusion assay

The antibacterial property of the CSNP-MMT-TiO_2 Nanocomposite was determined by using the bacterial species including the pathogenic bacteria such as Gram-positive *Staphylococcus aureus* and *Bacillus subtilus*, and Gram-negative *Escherichia coli*, *Enterobacter*, and *Pseudomonas fluorescens* by the well diffusion method. The different concentrations used were 0.01 mg and 0.1 mg for the identification of the antimicrobial activity of the above bacterial species and streptomycin is used as a control. All the plates were incubated at 37°C for 24 hours, and the zone of inhibition of bacteria was measured.

RESULT AND DISCUSSION

X-Ray Diffraction(XRD)

Fig. 1 shows the X-ray diffraction patterns of Chitosan and CSNP-MMT-TiO_2 Nanocomposite. The typical peaks of Chitosan (Fig. 1) appeared at 21.84° and 27.52°, while these peaks become weak in the XRD pattern. Other diffraction peaks in Fig. 2 are sharper and stronger at 25.38°, 37.84°, 48.10° and 62.71° were assigned to the (1 1 1), (3 1 1), (1 0 1), and (2 0 0) planes of distorted octahedral titanium dioxide can be indexed to the anatase TiO_2 with high crystallinity. All the diffraction peaks are in good agreement with those of cubic anatase structure of TiO_2 (JCPDS card 00-006-0696 and 00-003-1050).

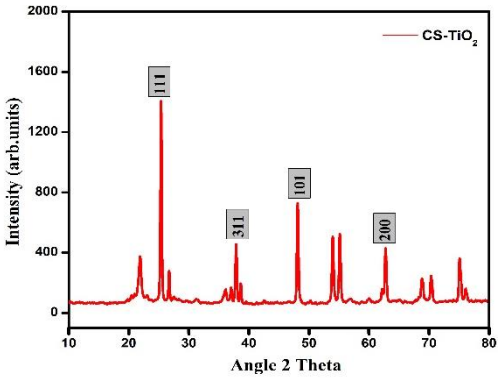

Fig. 1: X-Ray Diffraction (XRD) analysis of CSNP-MMT/TiO₂ Nanocomposite.

In comparison with the Chitosan NPs, the Chitosan peaks were found to become weak and shift right in the XRD pattern of CSNP-MMT-TiO_2 Nanocomposite [12]. The XRD pattern of the Nanocomposite shows the increased intensity of the TiO_2 peaks increasing with the amount of TiO_2. These results may be attributable to the increasing strength of the hydrogen bonds in the Chitosan complex while complexing with TiO_2 [1].

Fourier transforms infrared spectroscopy

Fig. 2 shows FT-IR spectra of the CSNP-MMT-TiO_2 Nanocomposite. The characteristic bands at 3436 to 2923 cm^{-1} are assigned to the N–H stretching with hydrogen bonded amino groups and C–H stretching vibration of alkyl, the band at 2013 cm^{-1} for C-H stretching of CH_2 in fatty acid, and the band at 1881 cm^{-1} for C≡C terminal alkynes[18]. The bands at 1700 cm^{-1} are attributed to the symmetric C=C stretching (conjugated) alkenes. The bands change compared to the pure CSNPs in the region from 800 to 400 cm^{-1} due to the presence of C-H bend (mono) aromatics, acetylenic C-H bend alkynes, C–Br stretch alkyl halides[19]. The broad peaks appearing at 1120 cm^{-1} are assigned to the stretching vibration of the C–N stretch aliphatic amines on the surface of CSNP-MMT-TiO_2 Nanocomposite. FT-IR analysis result reveals that the C–N stretch aliphatic amines inorganic network was bonded with CSNPs macromolecules by hydrogen bonding as well as covalent bonding in CSNP-MMT-TiO_2 Nanocomposite.

Dynamic light scattering

The size distribution of the CSNP-MMT/TiO_2 Nanocomposite was measured by Dynamic Light Scattering (DLS)

S.No	Peak (cm^{-1})	Functional Group
1	3436	N–H stretching with hydrogen bonded amino groups
2	2923	C–H stretching vibration of alkyl
3	2013	C-H stretching of CH_2 in fatty acid
4	1881	C≡C terminal alkynes
5	1700	C=C stretch (conjugated) alkenes
6	1120	C–N stretch aliphatic amines
7	792	C-H bend (mono) aromatics
8	623	acetylenic C-H bend alkynes
9	474	C–Br stretch alkyl halides

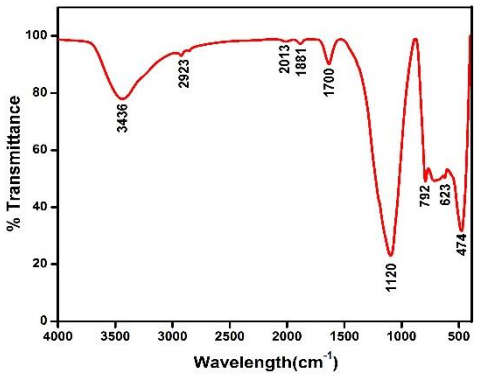

Fig. 2: FT-IR spectra of CSNP-MMT/TiO2 Nanocomposite.

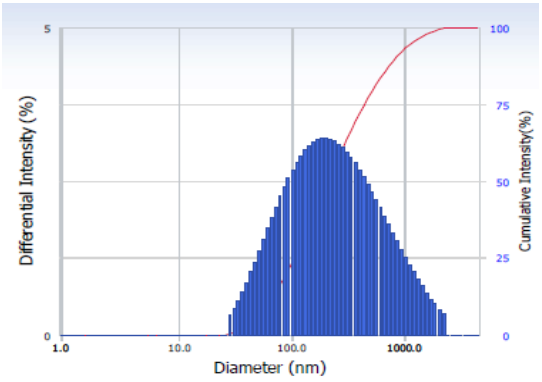

Fig. 3: The particle size and distribution of CSNP-MMT/TiO2 Nanocomposite.

as shown in Fig. 3. The DLS method examines the intensity of scattered light passing through a solution of nanoparticles [20]. The average size was measured from the majority of particle sizes of a sample. From the result, the average size distribution of the synthesized CSNP-MMT/TiO_2 Nanocomposite was observed at 62 nm.

Scanning electron microscopy

SEM micrographs illustrate the morphology of CSNP-MMT-TiO_2 Nanocomposite in Fig. 4. The CSNP were found to be freely distributed, providing a rough surface area to attach MMT-TiO2 Nanocomposite as shown in Fig. 4. It can be clearly seen that CSNP-MMT-TiO_2 Nanocomposite shows uneven Nanocomposite clusters with agglomerated and spherical shapes [21].

UV–Visible spectroscopy

The UV–Visible diffuse reflectance spectra of CSNP-MMT-TiO_2 Nanocomposite are shown in Fig. 5. The recorded UV–visible diffuse spectra are in the range between 200-1100 nm at room temperature. CSNP-MMT-TiO_2 shifts its absorption edge to a longer wavelength in the range 300-900 nm while CSNP-MMT-TiO_2 Nanocomposite has its absorption peak in the range 520 nm. The selected concentration of CSNP dopant in MMT and TiO_2 generates oxygen vacancies due to the charge compensation effect which allows the CSNPs to shift towards the visible range [15]. In agreement with the previous reports, the concentration of CSNPs has a band gap of 2.60 eV. Whereas the CSNP-MMT-TiO_2 shows absorption is in between 300-900 nm. The observed redshift for CSNPs was attributed to the existence of MMT and TiO_2 [22]. This emphasizes that the visible absorption phenomenon of CSNPs is closely associated with MMT and TiO_2 host lattice and in the presence of a high amount of TiO_2, significant changes can be seen.

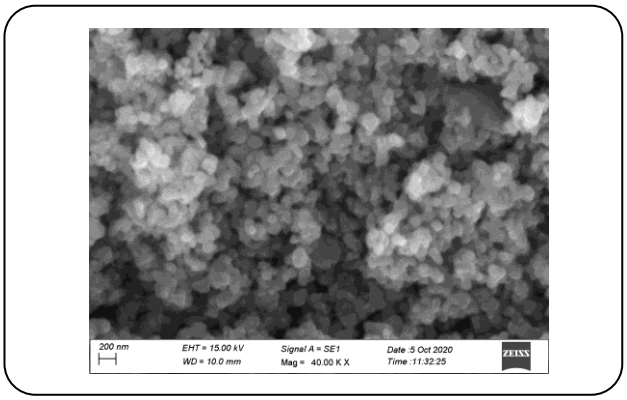

Fig. 4: Represents the SEM image of CSNP-MMT/TiO2 Nanocomposite

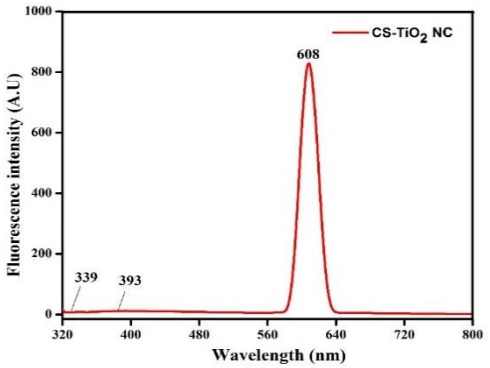

Fig. 6. Fluorescence spectra of CSNP- TiO_2-MMT.

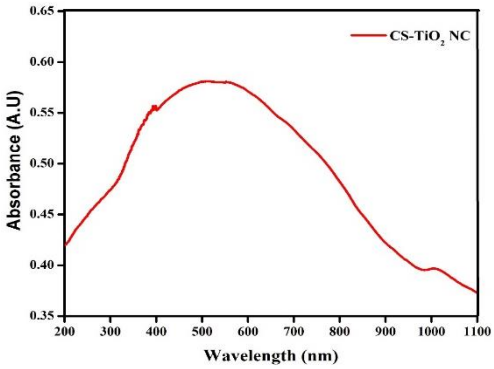

Fig. 5. Absorption spectra of CSNP-MMT/TiO_2 nanocomposite.

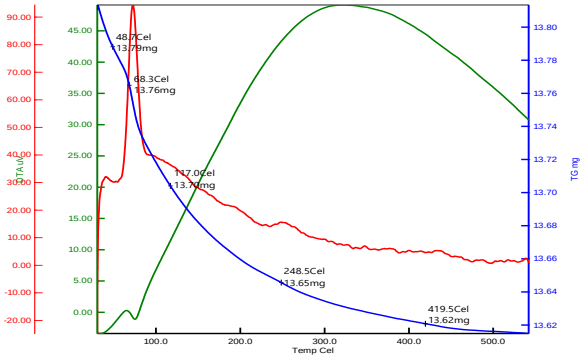

Fig. 7. TGA curve of CSNP-MMT/TiO_2 nanocomposite

FL spectroscopy

The fluorescence spectrum of CSNP-MMT-TiO_2 Nanocomposite is shown in Fig. 6. At the excitation wavelength of Fluorescence (FL) band appears at 608 nm, the maximum fluorescence peak of CSNP- TiO_2-MMT was found to be 393. These results indicate that the fluorescence emission band intensity and the absorption band of CSNP-MMT-TiO_2 Nanocomposite were concentration and particle size dependent[23]. The fluorescence spectra of CSNP-MMT-TiO_2 Nanocomposite present at a series of emissions in the domain 320 to 800 nm.

Thermogravimetric analysis

The thermal stability of the CSNP-MMT-TiO_2 Nanocomposite was measured using a thermal gravimetric analysis as shown in Fig. 7. For CSNP-MMT-TiO_2 Nanocomposite, weight loss took place in two clear stages. The first stage was observed at 10 °C and ended at 50 °C with a weight loss of 0.3 mg, which was assigned to the loss of water in CSNP-MMT-TiO_2 Nanocomposite. The second stage was observed at 50 °C and went on to 480 °C with a weight loss of 14 mg, which corresponded to the decomposition of CS and vaporization and elimination of volatile products [24]. The TG curve of the CSNP-MMT-TiO_2 also shows two distinct weight loss stages. The first step from 10 °C to 50 °C was characterized by a 0.3 mg weight loss inclusive of water loss this is endorsed to introduce the M–O network in the CSNP-MMT-TiO_2 Nanocomposite correlate with the IR spectrum analysis respectively. The second step at 50–480 °C is caused by the decomposition of the residual organic materials [25]. CSNP-MMT-TiO_2 completely decomposes at around 500 °C, permits to conclude that residue weight at 550 °C is of CSNP the remnant of CSNP-MMT-TiO_2 Nanocomposite.

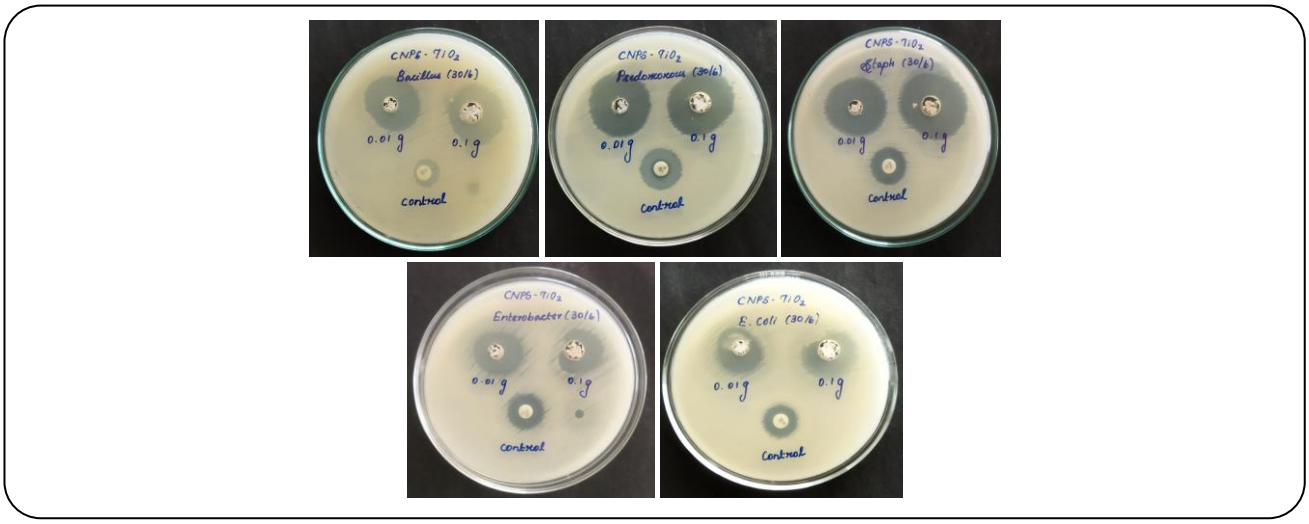

Fig. 8: Zone of inhibition of CSNP-MMT/TiO2 Nanocomposite using various bacterial strains.

It can be seen that CSNP-MMT-TiO_2 exhibited better thermal stability than the CSNPs.

Antibacterial activity

The goal of this work was to assess the synthesized CSNP-MMT/TiO_2 Nanocomposite with its antimicrobial activity and its dependence of that action on the chosen microbial species, namely, *staphylococcus aureus, Pseudomonas sp, Bacillus subtilis, Enterobacter and Escherichia coli.*

The different species of bacteria show a zone of inhibition in the well diffusion method of antimicrobial activity. The different patterns of the zone of inhibitions were observed in Fig.8. Synthesized CSNP-MMT/TiO_2 Nanocomposite showed antibacterial activity against both Gram-positive and negative bacteria. Pathogenic bacteria are grown in nutrient broth and 24 h culture of these strains was swabbed uniformly onto the individual plates containing muller hinton agar using sterile cotton swabs. About 5 wells were made and the purified CSNP-MMT/TiO_2 Nanocomposite at different weights like 0.01 g and 0.1 g were added into each well on all plates and streptomycin was used as control. The plates were incubated for 24 h at 37°C in an incubator. After incubation, the different levels of zone formation around the well were measured.

CONCLUSIONS

In summary, we have successfully prepared an effective antimicrobial CSNP-MMT/TiO_2 Nanocomposite with the help of sol–gel and precipitation method method. XRD and FTIR confirmed the CSNP-MMT/TiO_2 Nanocomposite characteristic featuring nanocrystalline TiO_2 in the tetragonal anatase phase. SEM analysis revealed the spherically agglomerated NPs size with an average mean diameter of 16 nm. The present study is an attempt to utilize visible light instead of only the UV range for CSNP-MMT/TiO_2 Nanocomposite. The presence of CSNP-MMT/TiO_2 played a vital role in altering the physiochemical and antimicrobial activity of CSNP-MMT/TiO_2. The optical band gap energy of CSNP-MMT/TiO_2 Nanocomposite shifted from UV region to visible light region as compared to CSNPs. The CSNP-MMT/TiO_2 Nanocomposite shows the best result and is 200 % more effective compared to positive control for antimicrobial application. In a two-component system where CSNP-MMT/TiO_2 Nanocomposite kills the bacteria and CSNP-MMT/TiO_2 Nanocomposite destructs the cell wall by electrostatic interaction and oxidative stress. Hence, the synergistic effects are the reason behind the enhanced antimicrobial activities where two components help each other through their individual killing mechanism. This paper provides a protocol for the synthesis of a new hybrid material that has antimicrobial activity.

Acknowledgments

I am E. Amutha (Register No: 19214542052003) acknowledges the Research center Sri Paramakalyani Centre of Excellence in Environmental Sciences, Manonmaniam Sundaranar University, Alwarkurichi, providing support for this research work.

Received : Oct. 29, 2021 ; Accepted : Feb. 14, 2022

REFERENCES

[1] Alagumuthu G., Kumar T.A., Synthesis and Characterization of Chitosan/TiO_2 Nanocomposites Using Liquid Phase Deposition Technique, *International Journal of NanoScience and Nanotechnology*, **4(1)**: 105-111 (2013).

[2] Bard A.J., "Integrated Chemical Systems: A Chemical Approach to Nanotechnology", John Wiley & Sons Inc., ISBN: 978-0-471-00733-3,342 (1994).

[3] Karaca S., Onal E.C., Acıslı O., Khataee A., Preparation of Chitosan Modified Montmorillonite Biocomposite for Sonocatalysis of Dyes: Parameters and Degradation Mechanism, *Materials Chemistry and Physics*, **260**: 124-125 (2021).

[4] Alshammari M.S., Essawy A.A., El-Nggar A.M., Sayyah S.M., Ultrasonic-Assisted Synthesis and Characterization of Chitosan-Graft-Substituted Polyanilines: Promise Bio-Based Nanoparticles for Dye Removal and Bacterial Disinfection, *Journal of Chemistry*, **32**: 97-184 (2020).

[5] Abdel Aziz M.S., Naguib H.F., Saad G.R., Nanocomposites Based on Chitosan-Graft-Poly(N-Vinyl-2-Pyrrolidone): Synthesis, Characterization, and Biological Activity, *International Journal of Polymeric Materials and Polymeric Biomaterials*, **64**: 578–586 (2015).

[6] Liu N., Chen X.G., Park H.J., Liu C.G., Liu C.S., Meng X.H., Yu L.J., Effect of MW and Concentration of Chitosan on Antibacterial Activity of *Escherichia coli*, *Carbohydrate Polymers*, **64**: 60–65 (2006).

[7] Jong-Whan Rhim., Seok-In Hong, Hwan-Man Park., Ng P.K.W., Preparation and Characterization of Chitosan-Based Nanocomposite Films with Antimicrobial Activity, *ACS Publications*, **54:** 16, 5814–5822 (2006).

[8] Peh K., Khan T., Chang H., Mechanical, Bioadhesive Strength and Biological Evaluations of Chitosan Films for Wound Dressing, *J. Pharm. Pharm. Sci.*, **3**: 303–311 (2000).

[9] Shabunin A.S., Yudin V.E., Dobrovolskaya I.P., Zinovyev E.V., Zubov V., Ivan'kova E.M., Morganti P., Composite Wound Dressing Based on Chitin/Chitosan Nanofibers: Processing and Biomedical Applications, *Cosmetics*, **6**: 16 (2019).

[10] Rehan M., El-Naggar M.E., Mashaly H.M., Wilken R., Nanocomposites Based on Chitosan/silver/clay for Durable Multi-Functional Properties of Cotton Fabrics, *Carbohydr. Polym.*, **182:** 29–41(2018).

[11] Chandrasekaran M., Kim K.D., Chun S.C., Antibacterial Activity of Chitosan Nanoparticles: A Review, *Processes*, **8:** 1173 (2020).

[12] Preethi S., Abarna K., Nithyasri M., Kishore P., Deepika K., Ranjith Kumar R., Bhuvaneshwari V., Bharathi D., Synthesis and Characterization of Chitosan/Zinc Oxide Nanocomposite for Antibacterial Activity onto Cotton Fabrics and Dye Degradation Applications, *International Journal of Biological Macromolecules*, **164**: 2779–2787(2020).

[13] Qi L., Xu Z., Jiang X., Hu C., Zou X., Qi L., Xu Z., Jiang X., Hu C., Zou X., Preparation and Antibacterial Activity of Chitosan Nanoparticles, *Carbohydrate Research*, **339**: 2693–700(2004).

[14] Pasaribu S.P., Kaban J., Ginting M., Sinaga K.R., Synthesis and Evaluation Antibacterial Activity of Phosphate Buffer Solution (pH 7.4) - Soluble Acylated Chitosan Derivative, *AIP Conference Proceedings*, **2049**: 020-025(2018).

[15] Habiba U., Joo T.C., Shezan S.K.A., Das R., Ang B.C., Afifi A.M., Synthesis and Characterization of Chitosan/TiO2 Nanocomposite for Adsorption of Congo Red, *DWT*, **164:** 361–367(2019).

[16] Taspika M., Desiati R.D., Mahardika M., Sugiarti E., Abral H., Influence of TiO2/Ag Particles on the Properties of Chitosan Film, *Adv. Nat. Sci: Nanosci. Nanotechnol*, **11**: 015-017(2020).

[17] Zafar N., Uzair B., Niazi M.B.K., Sajjad S., Samin G., Arshed M.J., Rafiq S., Fabrication & Characterization of Chitosan Coated Biologically Synthesized TiO2 Nanoparticles against PDR E. coli of Veterinary Origin, *Advances in Polymer Technology*, **84**: 56024 (2020).

[18] Bhumkar D.R., Pokharkar V.B., Studies on Effect of pH on Cross-Linking of Chitosan with Sodium Tripolyphosphate: A Technical Note, *AAPS PharmSciTech*, **7:** p. E138–E143(2006).

[19] Paluszkiewicz C., Stodolak E., Hasik M., Blazewicz M., FT-IR Study of Montmorillonite–Chitosan Nanocomposite Materials, *Spectrochimica Acta Part A: Molecular and Biomolecular Spectroscopy*, **79**: 784–788 (2011).

[20] Akbari B., Tavandashti M.P., Zandrahimi M., Particle Size Characterization of Nanoparticles – A Practical Approach, **8:** 9(2011).

[21] Khedr M.A., Waly A.I., Hafez A.I., Ali H., Synthesis of Modified Chitosan - Montmorillonite Nanocomposite, *Australian Journal of Basic and Applied Sciences*, **6(6)**: 216-226 (2012).

[22] Anaya-Esparza L.M., Ruvalcaba-Gómez J.M., Maytorena-Verdugo C.I., González-Silva N., Romero-Toledo R., Aguilera-Aguirre S., Pérez-Larios A., Montalvo-González E., Chitosan-TiO2: A Versatile Hybrid Composite, *Materials,* **13**: 811 (2020).

[23] Alba M.D., Cota A., Osuna F.J., Pavón E., Perdigón A.C., Raffin F., BioNanocomposites Based on Chitosan Intercalation in Designed Swelling High-Charged Micas, *Sci. Rep.*, **9**: 10265 (2019).

[24] Ali S.W., Joshi M., Rajendran S., Synthesis and Characterization of Chitosan Nanoparticles with Enhanced Antimicrobial Activity, *Int. J. Nanosci*, **10**: 979–984 (2011).

[25] Cremar L., Gutierrez J., Martinez J., Materon L., Gilkerson R., Xu F., Lozano K., Development of Antimicrobial Chitosan Based Nanofiber Dressings for Wound Healing Applications, *Nanomedicine Journal*, **5**: 6–14 (2018).

[37] Jayrajsinh S., Shankar G., Agrawal YK., Bakre L., Montmorillonite Nanoclay as a Multifaceted Drug-Delivery Carrier: A Review, *J. Drug Deliv. Sci. Technol.*, **39:** 200-209 (2017).

[38] Shunmugasamy VC., Xiang C., Gupta N., Clay/polymer Nanocomposites: Processing, Properties, and Applications, In: Kim C.-S., Randow C., Sano T., (Editors). "Hybrid and Hierarchical Composite Materials". Springer International Publishing; p. 161200 (2015).

[39] Müller K., Bugnicourt E., Latorre M., Jorda M., Echegoyen Sanz Y., Lagaron JM., et al. Review on the Processing and Properties of Polymer Nanocomposites and Nanocoatings and their Applications in the Packaging, Automotive and Solar Energy Fields, *Nanomaterials* **7(4)**: 74 (2017).